atmosphere

MDPI

Article

Patterns of Extreme Precipitation and Characteristics of Related Systems in the Northern Xinjiang Region

Rui Xu and Jie Ming *

Key Laboratory of Mesoscale Severe Weather (Ministry of Education), School of Atmospheric Sciences, Nanjing University, Nanjing 210023, China; mg1828024@smail.nju.edu.cn
* Correspondence: jming@nju.edu.cn

Abstract: Based on 40 years of daily precipitation, 272 extreme precipitation days in the Northern Xinjiang region are defined. Using the daily precipitation data on these days, four precipitation spatial patterns were obtained through principal component analysis. Then, daily-averaged reanalysis data were used to analyze the variations of synoptic systems on extreme precipitation days and the two days before and after. The rainfall centers shifted with the influential systems at 500 hPa. Water vapor of the western Tianshan type (Type WT) and the north of Northern Xinjiang type (Type NN) comes from the west, while vapor of the Central Tianshan type (Type CT) mainly comes from the east. In the east of Northern Xinjiang type (Type EN), water vapor converges from both sides. The centers of the upper-level jets are located west of 80° E in Type WT and CT. However, they are to the east of 80° E in the other types. This article summarizes the variations of the systems at 500 hPa, the South Asia High, the westerly jet, and the water vapor transport between the surface and 500 hPa in four types of patterns, and builds the conceptual model for each type. The models built can be applied to the heavy rainfall forecast of Northern Xinjiang.

Keywords: Northern Xinjiang; extreme precipitation; classification; conceptual model

Citation: Xu, R.; Ming, J. Patterns of Extreme Precipitation and Characteristics of Related Systems in the Northern Xinjiang Region. *Atmosphere* **2021**, *12*, 358. https://doi.org/10.3390/atmos12030358

Academic Editors: Wen Zhou and Anthony R. Lupo

Received: 23 February 2021
Accepted: 6 March 2021
Published: 9 March 2021

1. Introduction

Xinjiang is located in the middle of the Eurasian continent, far away from the sea and surrounded by mountains. Climatologically, summer precipitation accounts for 54.4% of the total rainfall in the whole year, indicating the dominant role of severe rainfall in the summer on the total annual rainfall [1]. Although rainstorms occur infrequently (two to three each year) in the arid and semi-arid areas of Xinjiang, they can induce huge losses [2]. The catastrophic rainstorms and floods in Xinjiang happen mostly in the summer, while their induced loss has a significant positive correlation with the annual precipitation in Xinjiang [3,4]. Xinjiang is divided by the Tianshan Mountains into northern and southern parts, between which there are significant differences in climate [5], and especially in precipitation. The strong signals of climatic shifting from a dry to a humid pattern have been observed in Northern Xinjiang since the late 1980s [6].

There are many studies of the large-scale synoptic systems related to precipitation in Xinjiang. Zhao et al. [7] found that the most frequent pattern for the South Asia High in the last 35 years was the Iran High pattern. When the center of the Iran High pattern shifted further west, it caused more summer precipitation in Xinjiang, and vice versa. Yang et al. [8] studied the precipitation in July and August and showed that the South Asia High exhibited a two-center pattern in high-rainfall years. According to Zhang et al. [9], the ridge line of the South Asia High is closely related to precipitation in the northwest of China. A southward migration of the monthly mean ridge line increases precipitation over Northwest China. The strengthened subtropical westerly jet over Western and Central Asia is another key atmospheric system affecting summer rainfall over Xinjiang [8,10]. Zhao et al. [11] pointed out that the north–south oscillation of the jet had an impact on precipitation. When the jet position is further south, the anomalous southwesterly flow is favorable for the

southwestward transport of warm and wet air from low latitudes into northern Xinjiang, triggering rainfall. The secondary circulation generated by the subtropical westerly jet is the other important system affecting precipitation in Xinjiang [5,12]. At the 500 hPa level, when a trough or vortex exists in Central Asia between the Iran subtropical high and the western Pacific subtropical high, heavy rainfall happens more frequently in Xinjiang [5,12]. Through investigation of the anomalies of geopotential height at 500 hPa, Wang et al. [13] found that the enhancement of the Ural Mountain ridge favored the increase of precipitation in Xinjiang. It can be seen that the South Asia High, westerly jet, and influential systems at 500 hPa have a strong modulation on precipitation in Xinjiang.

Many studies focus on water vapor transport in Xinjiang. Dai et al. [14] pointed out that water vapor was mainly transported from the west due to the westerlies. Water vapor sources in Xinjiang are mainly lakes or oceans to the west of Xinjiang, such as the Aral Sea, the Caspian Sea, Lake Balkhash, the North Atlantic, and the Arctic Ocean [15,16]. In the summer, the North Atlantic and the Arctic Ocean are the main sources [17,18]. Furthermore, part of the water vapor transferred to Central Asia originates from tropical areas like the Indian Ocean [19,20]. Due to the blocking effect of the Tibetan Plateau, only a small part of the water vapor from the Indian Ocean can reach the Xinjiang region, and water vapor transport is the largest in the middle troposphere [21,22]. Also, associated with the subtropical high extending northward and westward, water vapor in eastern China can be transported into Xinjiang from the east through the Hexi Corridor [23,24]. These results show that water vapor sources vary in different synoptic backgrounds.

The climatic characteristics in Xinjiang were investigated in previous studies that analyzed the rainfall-related systems and water vapor transport separately. However, few of them considered the characteristics in rainfall-related systems and water vapor transport together, which are investigated in the present study. Based on the precipitation data of the Northern Xinjiang region in the past 40 years, this study focuses on the regional characteristics of summer heavy rainfall in Northern Xinjiang. Using the method of principal component analysis, precipitation in 272 extreme precipitation days in the Northern Xinjiang region are first classified into four types. The reanalysis data of each type is then analyzed in order to study the characteristics of the related systems and variables mentioned in the existing research. Finally, a conceptual model is built for each type, which can be applied to heavy rainfall forecasts in the Northern Xinjiang region. Section 2 introduces the observational and reanalysis data, as well as the methods used in the following parts. Section 3.1 shows the classification results of heavy rainfall patterns in the Northern Xinjiang region. Section 3.2 further analyzes the variations and characteristics of the related variables of each type. Section 3.3 focuses on building the typical configuration of the conceptual model for each type. Section 4 provides a summary of this study.

2. Materials and Methods

2.1. Data

Daily precipitation data were collected by the Xinjiang Meteorological Information Center at 52 stations in northern Xinjiang from June to August 1979–2018. The reanalysis data was collected from the European Centre for Medium-Range Weather Forecasts (ECMWF) official website (https://www.ecmwf.int/en/forecasts/datasets/browse-reanalysis-datasets) (accessed on 8 March 2021), including daily averaged ECMWF reanalysis interim (ERA-interim) data with a horizontal resolution of 1.5° × 1.5° [25], and ECMWF reanalysis version5 (ERA5) hourly data with a resolution of 0.25° × 0.25° [26]. The analyzed variables include geopotential height at 500 hPa, wind field at 200 hPa, and specific humidity between the surface and 500 hPa. ERA-interim reanalysis data were used in the composite analysis in Section 3.2. In order to obtain a finer structure of the systems when building conceptual models in Section 3.3, we used ERA5 data because of its finer resolution. We compared both sets of data and found no distinguishable differences between them when building conceptual models.

2.2. Methods

2.2.1. Definition of Extreme Precipitation Days in the Northern Xinjiang Region

The Northern Xinjiang region (as shown in Figure 1) is defined as the region north of 43° N, west of 91.5° E, and inside the Chinese border. Based on the daily precipitation in the summers of 1979–2018, extreme precipitation days are defined as when more than 20% of stations in the Northern Xinjiang region experienced precipitation above 95% percentile, and when more than 50% of stations had precipitation [27]. In total, there were 272 extreme precipitation days in the Northern Xinjiang region during the past 40 years.

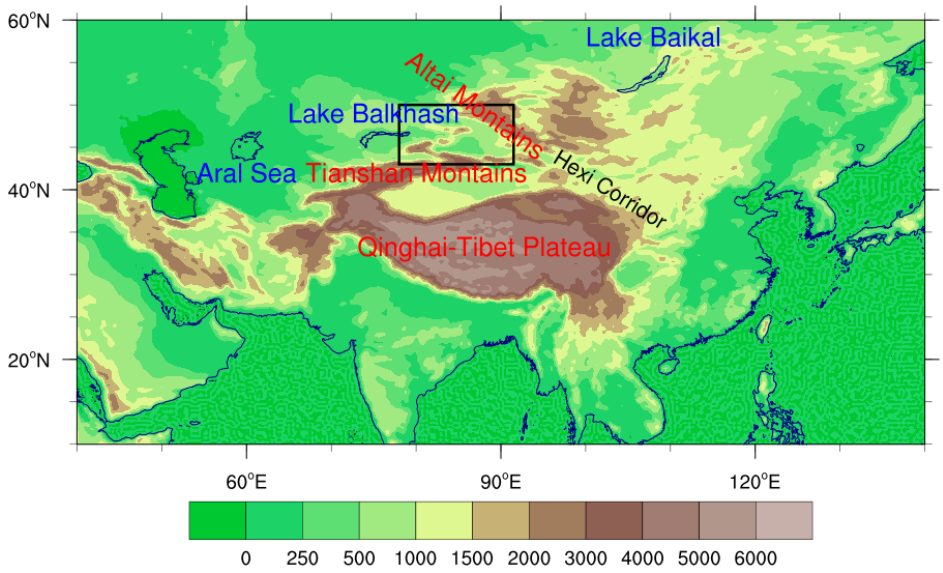

Figure 1. Topography of the surrounding area of the Northern Xinjiang region (Unit: m). The black box represents the location of the Northern Xinjiang region.

2.2.2. Objective Synoptic Classification Method

The obliquely rotated principal component analysis (PCA) in T mode (PCT hereafter) was applied to the daily precipitation station data to classify different synoptic patterns in this study. The difference between PCT and PCA is that the input data was processed so that the columns of the data represent the time series and the rows represent the grid data. After processing the PCA, an oblique rotation according to Richman [28] was applied to a few of the retained leading components. Each pattern was classified by the type for which it had the highest loading. The advantage of this method lies in its higher stability in time and space. For more details of this method, please refer to Huth [29,30].

This method proves to be a valuable tool when studying the synoptic characteristics of Eastern China. Li et al. [31] used classification to analyze the long-term trends of hail day frequency in mainland China and associated changes in the atmospheric circulation patterns. This method was also used to analyze the circulation characteristics of the Pearl River Delta in Rao et al. [32]. In theory, a similar study conducted in Xinjiang should bring fruitful results.

3. Results

3.1. Objective Classification of Extreme Precipitation in the Northern Xinjiang Region

Firstly, we studied the 40-year climatic features of precipitation in the Northern Xinjiang region (Figure 2). Greater daily-averaged precipitations in the Northern Xinjiang region were concentrated over two regions. One was over the area of 43–45° N, 80–90° E, while the other was near the Altai Mountains. According to 95th percentile rainfall, the center with heavy rains in the Northern Xinjiang region is consistent with the center with the greater daily-averaged precipitation. Large rainfalls also existed near 90° E, east

of the aforementioned center. The rainfall center on extreme precipitation days was also similar to the centers mentioned above. The difference is that the precipitation at the east of the center was larger than that at the west. In a word, the rainfall centers of daily-averaged precipitation, 95th percentile of daily precipitation, and extreme precipitation in the Northern Xinjiang region occurred in almost the same area.

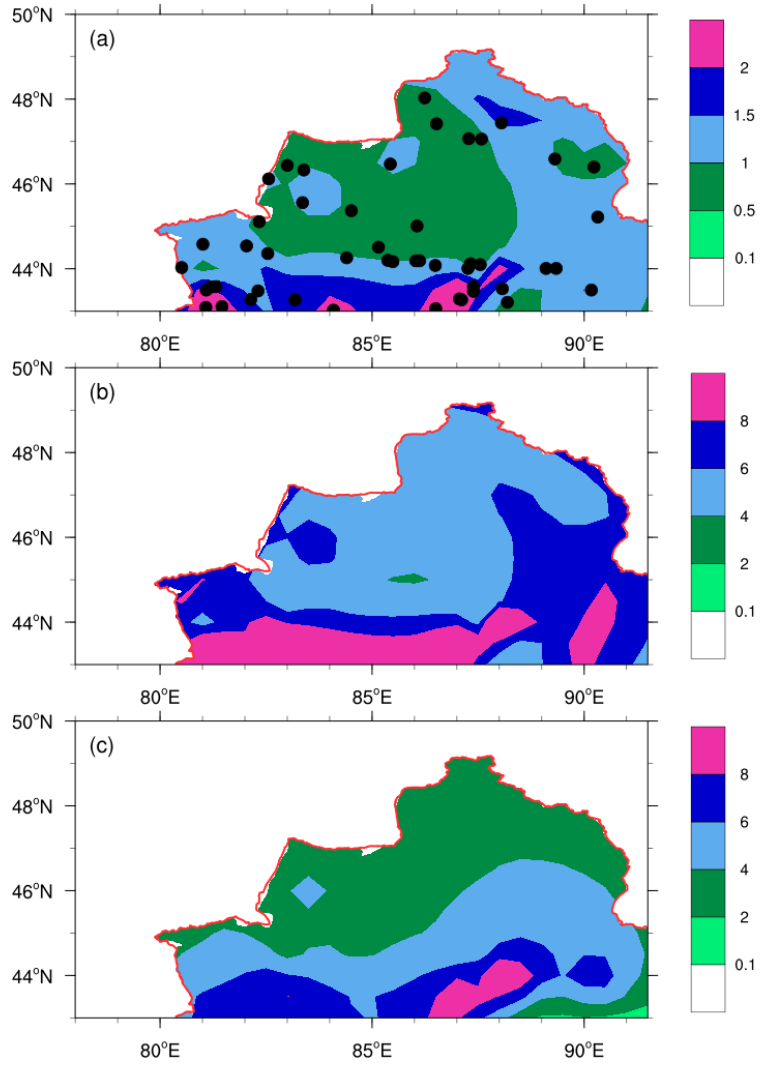

Figure 2. Precipitation in the Northern Xinjiang region in 1979–2018 (Unit: mm). (**a**) daily-averaged precipitation, with black dots indicating the locations of the observational stations; (**b**) 95th percentile of daily rainfall; (**c**) daily-averaged precipitation on extreme precipitation days.

In order to study the distribution of extreme precipitation in the Northern Xinjiang region, precipitation data of the selected days with extreme precipitations in the Northern Xinjiang region were used to conduct an objective classification through PCT (Figure 3). Ranked by their occurrence frequencies, the different types identified were: western Tianshan type (Type WT), north of Northern Xinjiang type (Type NN), east of Northern Xinjiang type (Type EN), and Central Tianshan type (Type CT). Since the case amount in type 5 was much less than those in other types, type 5 is not considered in the following discussion.

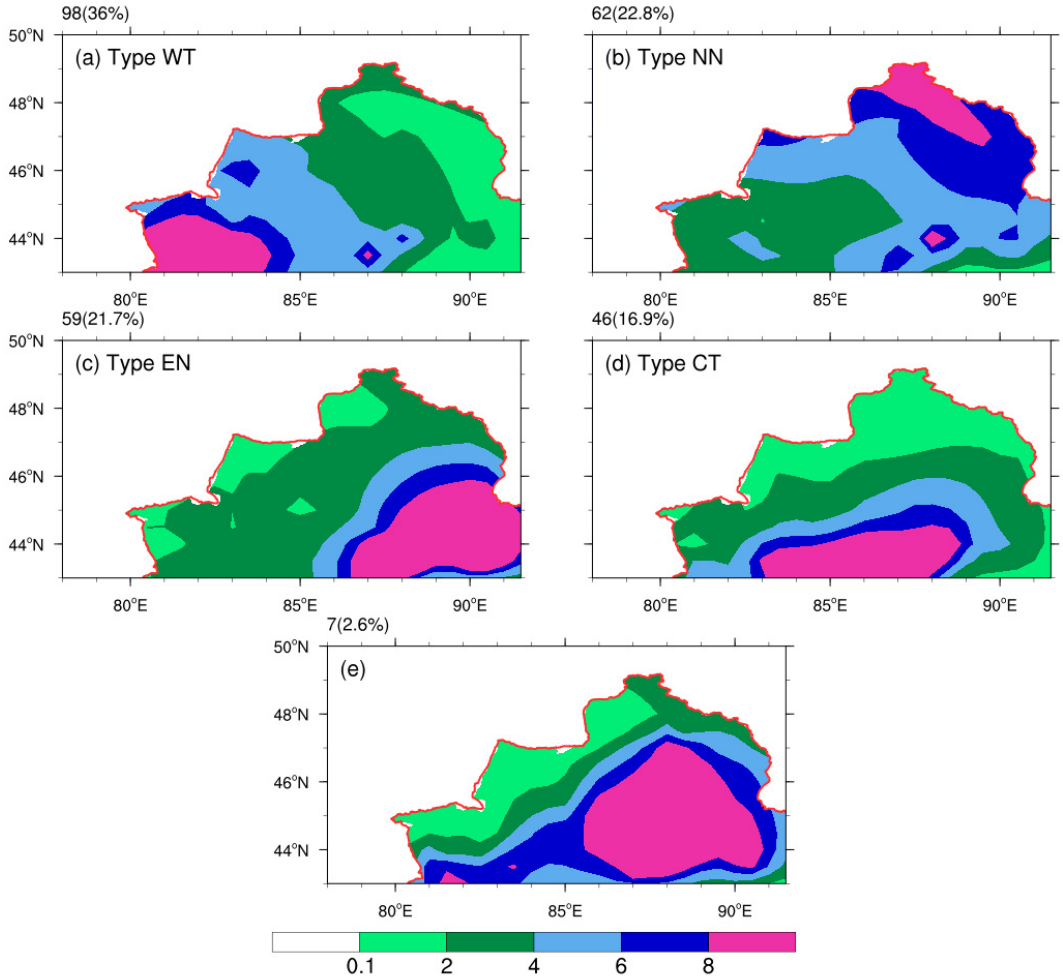

Figure 3. Results of the objective classification of daily precipitation of extreme process precipitation in the Northern Xinjiang region during summer in 1979–2018 (Unit: mm). The number on the upper left represents the number and percentage of occurrences. (**a**) Type WT; (**b**) Type NN; (**c**) Type EN; (**d**) Type CT; (**e**) Type 5.

3.2. Distribution of Variables of Extreme Precipitation in the Northern Xinjiang Region

Based on the results of our classification, variations in the weather systems related to the extreme precipitation were summarized by analyzing environmental variables at different levels before and after each rainfall case. The variables concerned included the geopotential height at 500 hPa (Z500), the water vapor flux between the surface and 500 hPa (Q), and the zonal wind speed at 200 hPa (U200), which were used to describe the variations of mid-level weather systems, middle- and lower-level water vapor transport, and upper-level jets, respectively. The anomalies of these variables were obtained by subtracting their average values on that day during the previous 40 years.

According to the precipitation center location, the rainfall distribution of Type WT was similar to that of the climate average. Therefore, it was easier to compare Type WT with the other three types (Types NN, EN, and CT) and to analyze the variations of anomaly fields to find the characteristics of the individual types.

3.2.1. Variations of the Geopotential Height Anomaly Field at 500 hPa

In Type WT (Figure 4), which had the highest occurrence frequency, the negative anomalous geopotential height at 500 hPa moved eastward and strengthened to the north of the Aral Sea. This center reached its peak at Lake Balkhash on the extreme precipitation day and then weakened rapidly. The centers of positive anomalies moved eastward along

with the negative anomalies. The one on the west side weakens continuously while the eastern one strengthens gradually.

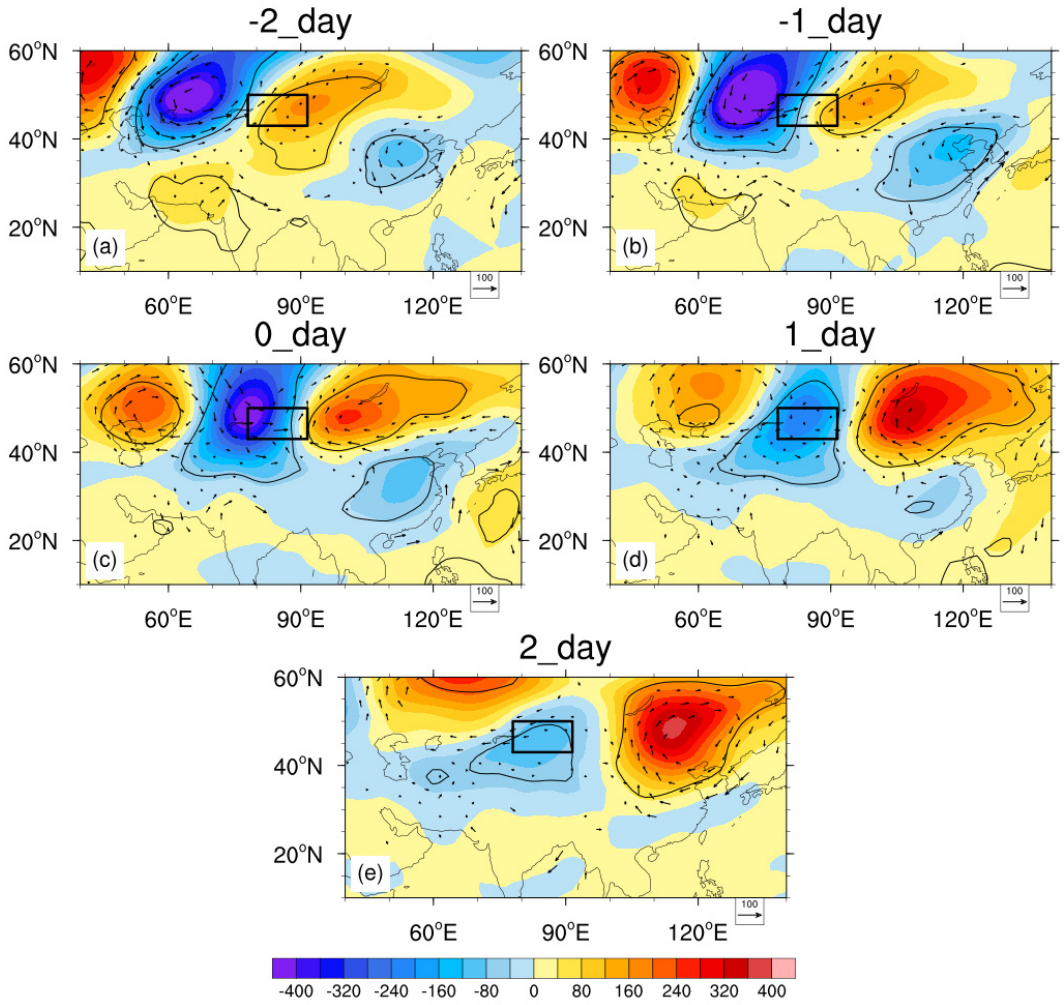

Figure 4. Composition of Z500 (contour) and Q anomaly (arrow) of Type WT on the extreme precipitation day and two days before and after (**a**–**e**) in the summers of 1979–2018 (Unit: gpm). The black box represents the location of the Northern Xinjiang region. The region over the 95% significant confidence level of geopotential height is circled with black lines, and only the part over the 95% significant confidence level of surface water vapor flux is shown.

As Figure 5 shows, the centers of negative anomalies in Type NN were first located at the northwest of Lake Balkhash and Lake Baikal, then merged gradually at the west of the Northern Xinjiang region before moving eastward and strengthening. After reaching the north of Xinjiang on the extreme precipitation day, the merging center continuously moved eastward and weakened gradually. Compared with Type WT, the intensity of negative anomaly was stronger (weaker) before (after) the day, whereas the intensity of the positive anomaly was weaker than that found in Type WT. The western one strengthened when moving eastward, and the eastern one weakened when moving eastward. It can be seen that the locations of ridge and trough or vortex at 500 hPa were more eastward than those in Type WT. The intensity of the low was weaker (stronger) before (after) rainfall, while the intensity of the high was weaker.

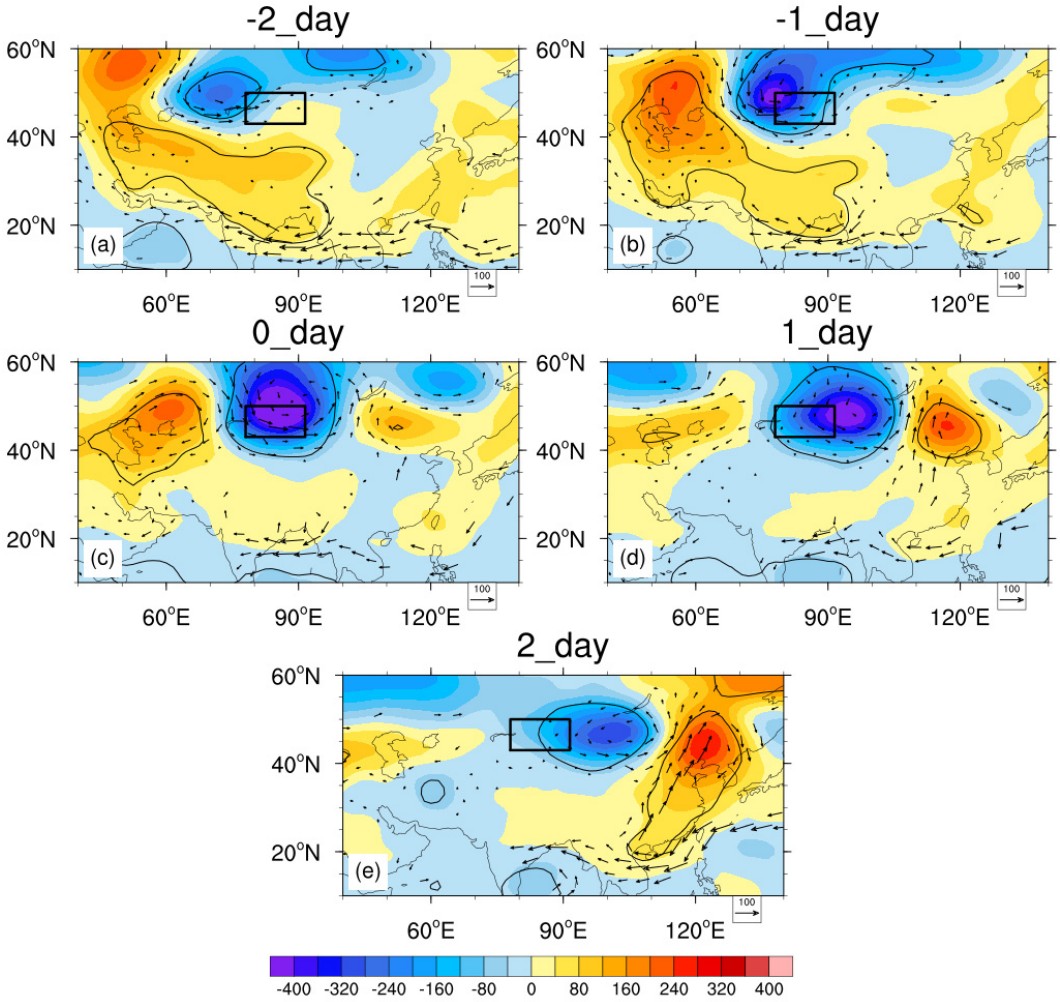

Figure 5. Composition of Z500 (contour) and Q anomaly (arrow) of Type NN on the extreme precipitation day and two days before and after (**a**–**e**) in summers of 1979–2018 (Unit: gpm). The black box represents the location of the Northern Xinjiang region. The region over the 95% significant confidence level of geopotential height is circled with black lines, and only the part over the 95% significant confidence level of surface water vapor flux is shown.

In Type EN (Figure 6), the negative anomaly moved eastward and strengthened at the northwest side of Lake Balkhash. The negative anomaly reached the north of Xinjiang on the extreme precipitation day, and then rapidly weakened while moving eastward. The positive anomalies moved eastward with the negative anomaly. The positive anomaly to the west slightly weakened while the positive anomaly to the east slightly strengthened. Compared with Type WT, the center of the anomalies in the eastern part of the Northern Xinjiang region was shifted more southward and eastward. The western and eastern centers of negative anomalies were weaker and stronger, respectively. It can be seen that the locations of ridge and trough or vortex at 500 hPa in Type EN migrated more southward and eastward than those in Type WT. The intensity of the low was significantly weaker, while the upstream high was stronger.

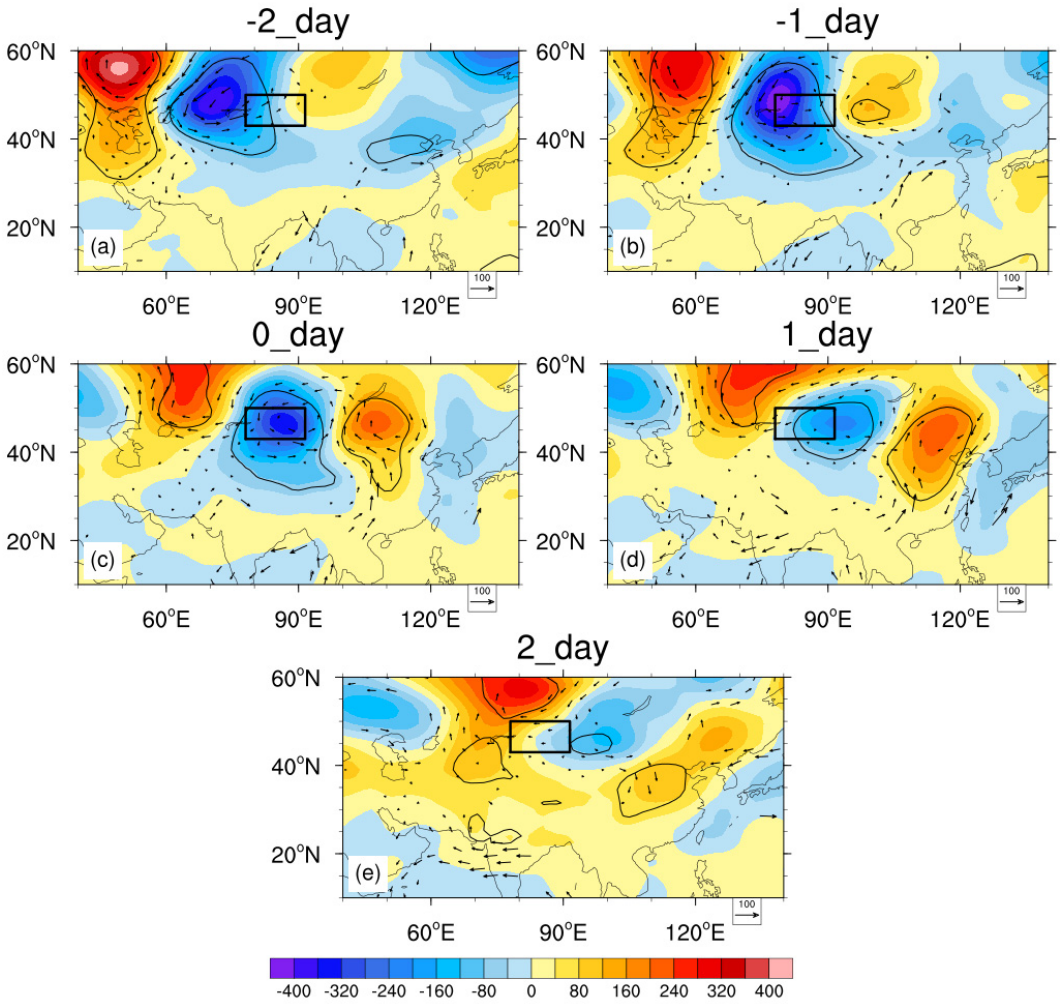

Figure 6. Composition of Z500 (contour) and Q anomaly (arrow) of Type EN on the extreme precipitation day and two days before and after (**a**–**e**) in the summers of 1979–2018 (Unit: gpm). The black box represents the location of the Northern Xinjiang region. The region over the 95% significant confidence level of geopotential height is circled with black lines, and only the part over the 95% significant confidence level of surface water vapor flux is shown.

As shown in Figure 7, the negative anomaly in Type CT was located more eastward compared to that of Type WT, but with a weakened intensity. The negative anomaly reached the valley of the Tianshan Mountains on the extreme precipitation day, and then continued to weaken and moved slightly eastward. The positive anomaly to the west moved eastward with the negative anomaly and gradually moved northward. The positive anomaly to the east was strengthened and stabilized south of Lake Baikal. The centers of the anomalies in Type CT were located more eastward than those in Type WT. It can be seen that the locations of the ridge and trough or vortex on the 500 hPa in Type CT were to the east of those in Type WT, while the intensity of the downstream high was obviously stronger.

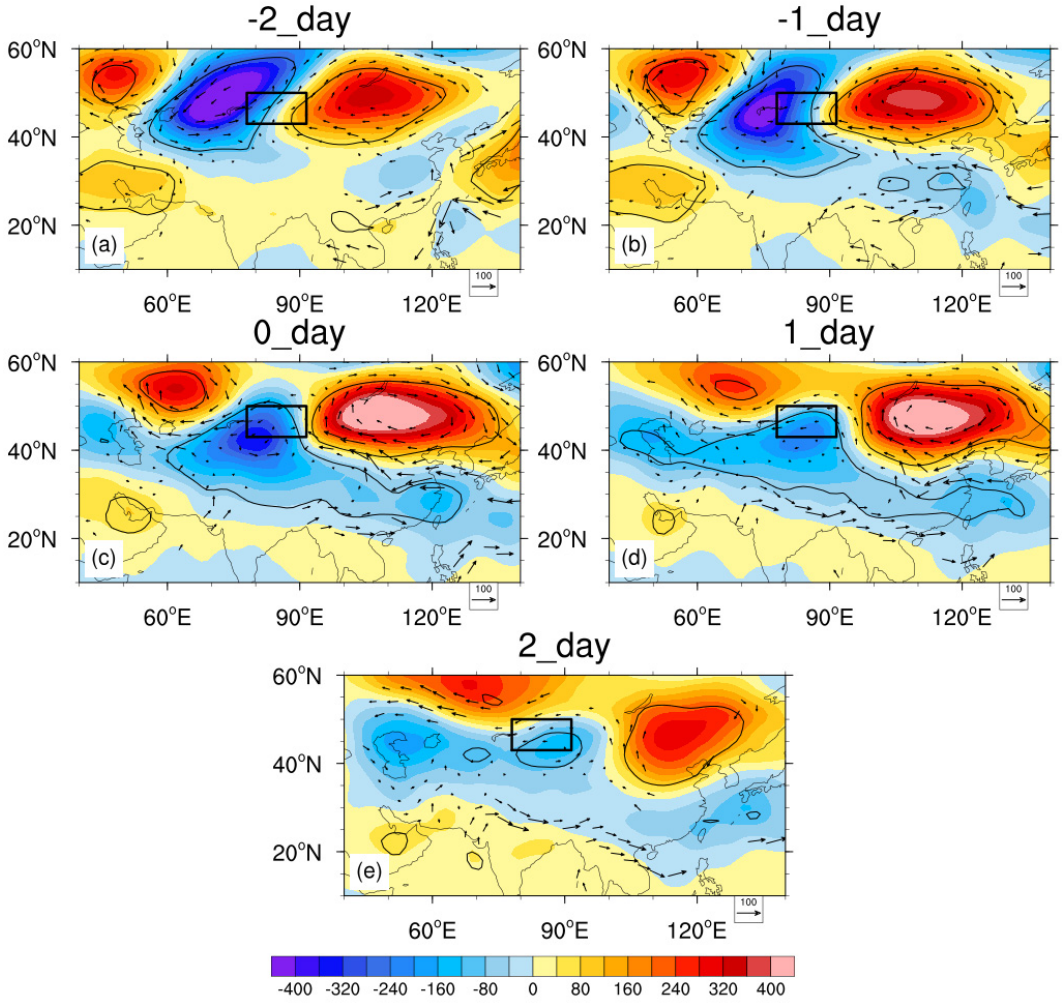

Figure 7. Composition of Z500 (contour) and Q anomaly (arrow) of Type CT on the extreme precipitation day and two days before and after (**a**–**e**) in the summers of 1979–2018 (Unit: gpm). The black box represents the location of the Northern Xinjiang region. The region over the 95% significant confidence level of geopotential height is circled with black lines, and only the part over the 95% significant confidence level of surface water vapor flux is shown.

3.2.2. Variations of Water Vapor Flux Anomaly Field from the Surface to 500 hPa

Water vapor transport is another essential ingredient for precipitation. Therefore, we need to discuss the variations in the water vapor flux between the surface and 500 hPa. On the day of the extreme precipitation and the day before, in Type WT (Figure 4), a large amount of water vapor was transferred to the valley of the Tianshan Mountains from the west and northwest of Xinjiang. In Type NN (Figure 5), water vapor was mainly transported to the northern part of the Northern Xinjiang region from the northwest side of Xinjiang. Water vapor flux has a tendency to form a vortex, with its center located between the Northern Xinjiang region and Lake Baikal. In Type EN (Figure 6), on the day before, water vapor originated from the northwest and southeast and converged in the eastern part of the Northern Xinjiang region, forming a vortex on the extreme precipitation day. The vortex center was located more southward compared to Type NN in the same period. On the day of the extreme precipitation and the day before, in Type CT (Figure 7), water vapor from the west and the east converged in the central part of the Tianshan Mountains.

3.2.3. Variations of Zonal Wind Anomaly Field at 200 hPa

The positive anomalies of the 200 hPa zonal wind in Type WT (Figure 8) were located in the north and southwest of the Northern Xinjiang region, and gradually moved eastward.

They strengthened before the occurrence of extreme precipitation and then weakened. At the same time, there was a negative anomaly in the northwest of the Northern Xinjiang region, which gradually weakened and moves eastward, while the center on the east side slightly strengthened during its eastward movement.

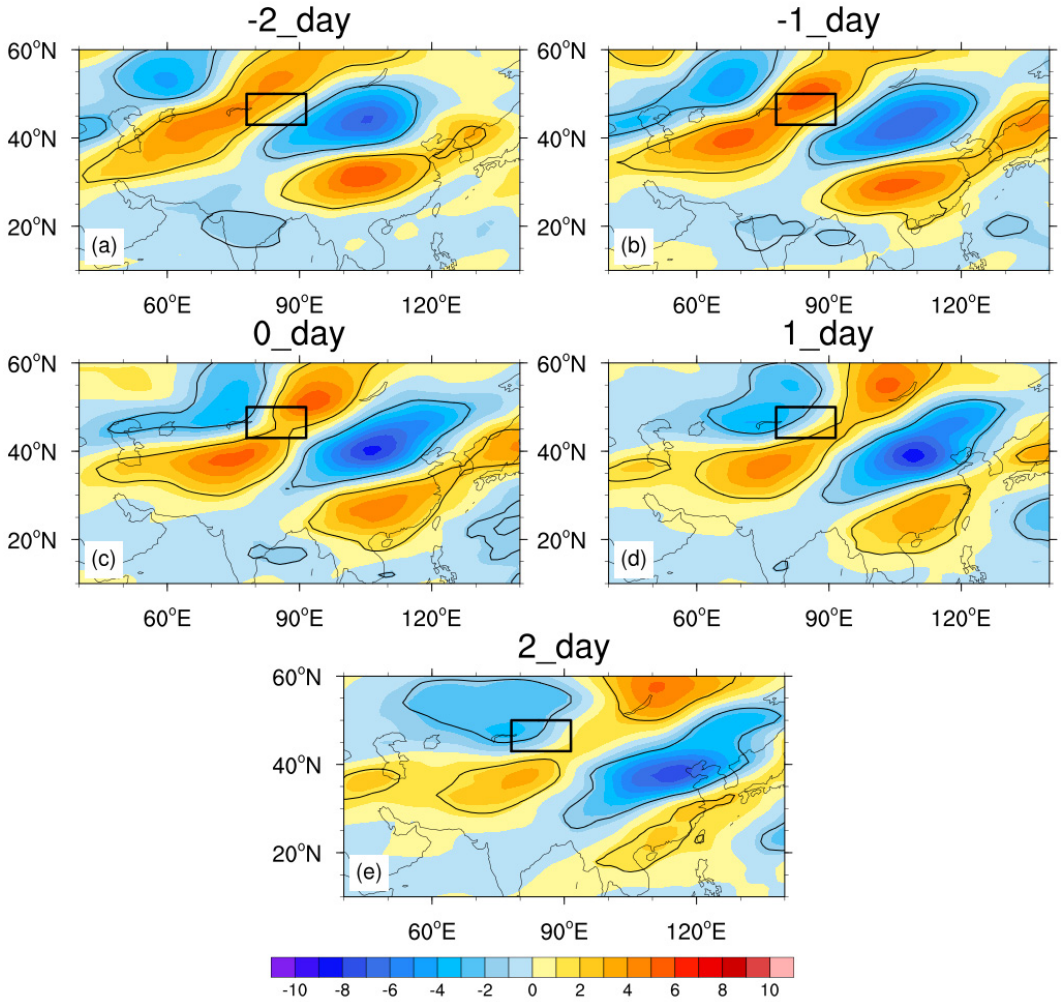

Figure 8. Composition of U200 anomaly of Type WT on the extreme precipitation day and the two days before and after (**a**–**e**) in the summers of 1979–2018 (Unit: m/s). The black box represents the location of the Northern Xinjiang region, and the region over the 95% significant confidence level is circled with black lines.

Compared with Type WT, the intensity of positive anomalies in Type NN (Figure 9) was weaker, and it moved eastward at a faster speed. Before rainfall, the positive anomaly appeared near the western part of the Northern Xinjiang region, and the northern part of the anomaly strengthened and moved eastward over time. The negative (positive) anomaly gradually appeared on the north (south) side of North Xinjiang and strengthened. After precipitation, the positive anomaly reached the north side of the Caspian Sea. That is to say, the intensity of the upper-level jet in the eastern part of the Northern Xinjiang region was weaker than that in Type WT, and the jet center moved eastward at a greater speed.

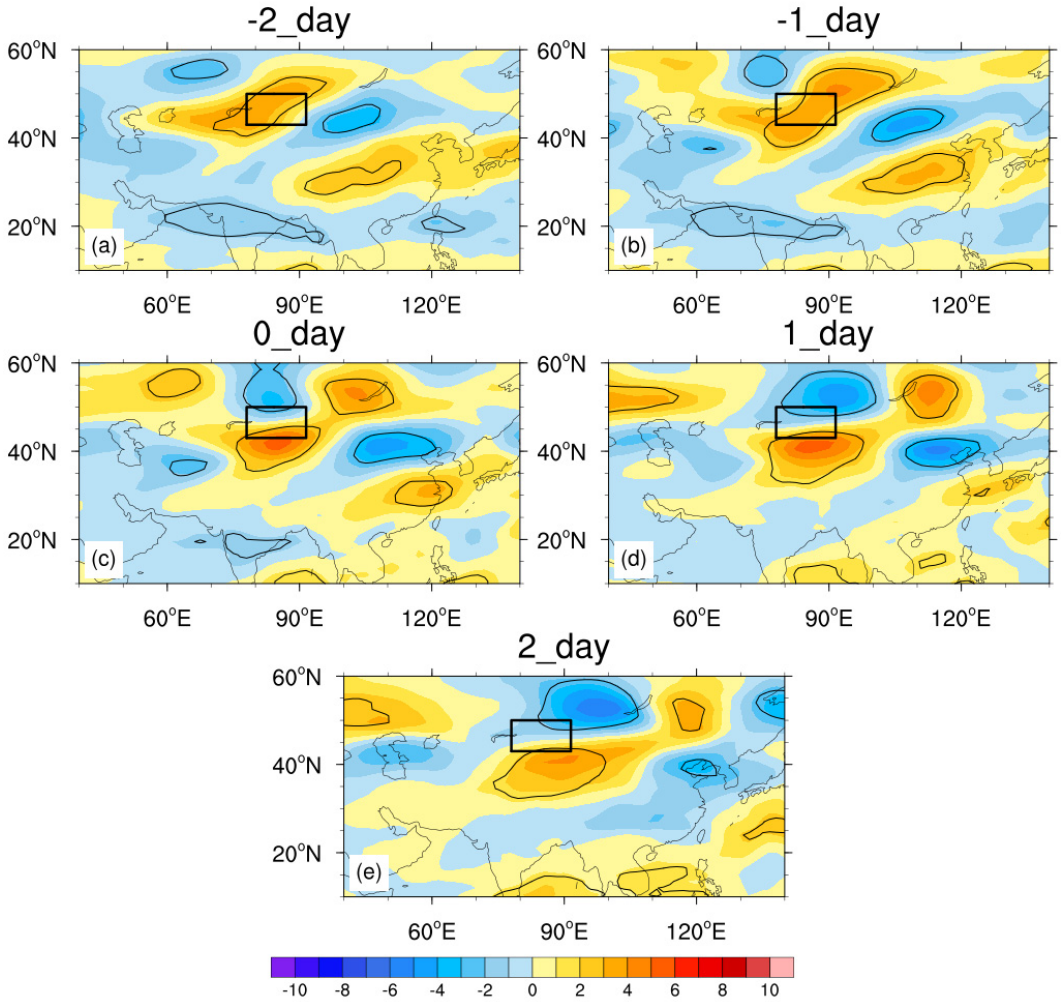

Figure 9. Composition of U200 anomaly of Type NN on the extreme precipitation day and the two days before and after (**a**–**e**) in the summers of 1979–2018 (Unit: m/s). The black box represents the location of the Northern Xinjiang region, and the region over the 95% significant confidence level is circled with black lines.

Compared with the former two types, the intensity of the positive anomaly in Type EN (Figure 10) was weaker, and the eastward-moving speed was faster. The day before the extreme precipitation, the positive anomaly was located near 40° N at the southwest side of the Northern Xinjiang region, and gradually weakened and moved eastward. At the same time, the negative anomaly appeared on the northwest side of Lake Balkhash and gradually moved eastward. Also, a positive anomaly appeared in the downstream area, which strengthened first and then weakened. That is to say, the intensity of the upper-level jet in Type EN was weaker than that in Type WT, and the jet center moved faster.

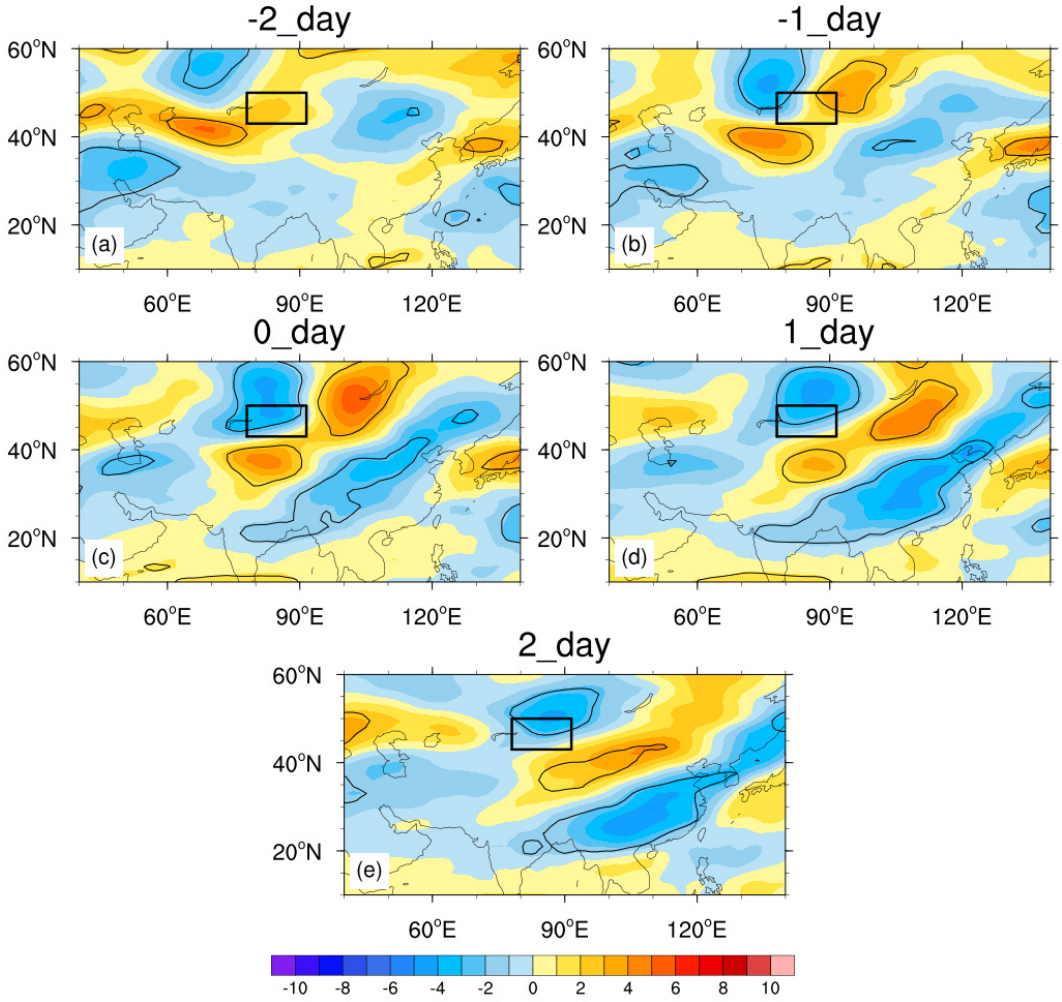

Figure 10. Composition of U200 anomaly of Type EN on the extreme precipitation day and the two days before and after (**a**–**e**) in the summers of 1979–2018 (Unit: m/s). The black box represents the location of the Northern Xinjiang region, and the region over the 95% significant confidence level is circled with black lines.

Finally, in Type CT (Figure 11), the field exhibited a saddle-shaped distribution with the Northern Xinjiang region located in the middle. The positive anomaly was in the southwest and northeast of North Xinjiang, while the negative anomaly in the southeast and northwest of North Xinjiang gradually moved eastward. The west center strengthened before precipitation and then weakened, while the center in the east continuously strengthened. Compared with Type WT, the center in Type CT was stronger and was located more southward before the extreme precipitation. The westerly jet in Type CT was more southward and stronger.

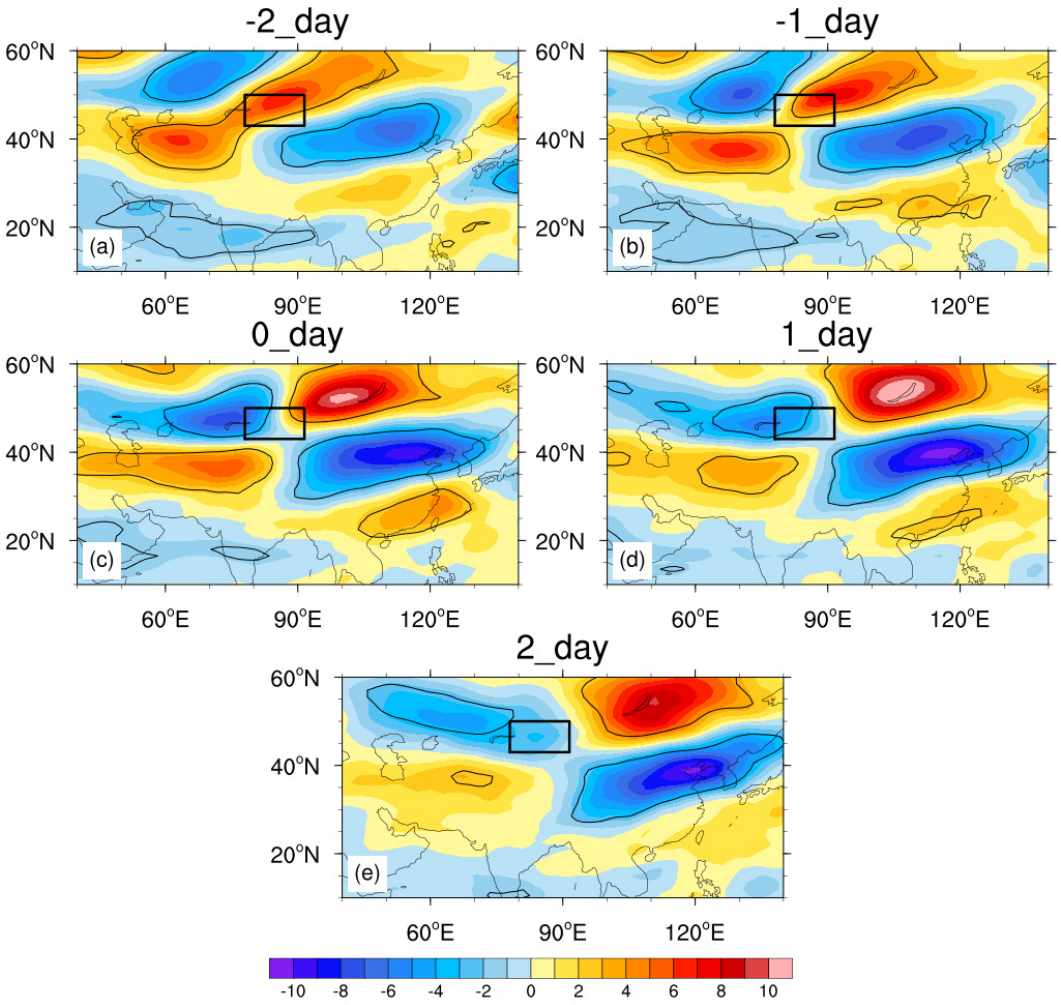

Figure 11. Composition of U200 anomaly of Type CT on the extreme precipitation day and the two days before and after (**a**–**e**) in the summers of 1979–2018 (Unit: m/s). The black box represents the location of the Northern Xinjiang region, and the region over the 95% significant confidence level is circled with black lines.

3.3. Configuration of Typical Systems

According to the results above, we can see that distribution of the variables in each type of extreme precipitation had its own distinguishable features. We further selected the cases with the largest daily precipitation at a single station in each year and analyzed the development of the influential systems and the related variables on the extreme precipitation day and the two days before and after. Based on the reanalysis data of ERA5, the variations in the 500 hPa weather systems, the westerly jet, and water vapor transport in four types of precipitation are summarized. Although the composite analyses conducted on geopotential height at 100 hPa showed no significant differences, the variations of the South Asia High are summarized because there are still some distinguishable features in the typical cases of different types. All of the variations are shown in 3D models in the style of Sun & Zhao [33], which helps present the configuration of systems on the high and low levels and makes it easy for us to distinguish each system on different levels. With notes on every level, 3D conceptual models can describe the location of the systems more clearly than 2D maps. If the correlation coefficient at 500 hPa between the typical situation in the conceptual model and one of the cases was more than 0.5, then the case was categorized to be similar to the typical case.

13 cases in Type WT are selected. On one hand, 9 of them are similar to the typical case of configuration WT1 (Figure 12a). In this configuration, the trough at 500 hPa is located in

Siberia and moves eastward. On the extreme precipitation day, it appears at the north of Lake Balkhash. The South Asia high appears with two centers at about 55° E and 95° E, respectively, and the westerly jet is averagely located at 40° N. Water vapor is transferred to the Valley of Tianshan Mountains from the west of Xinjiang.

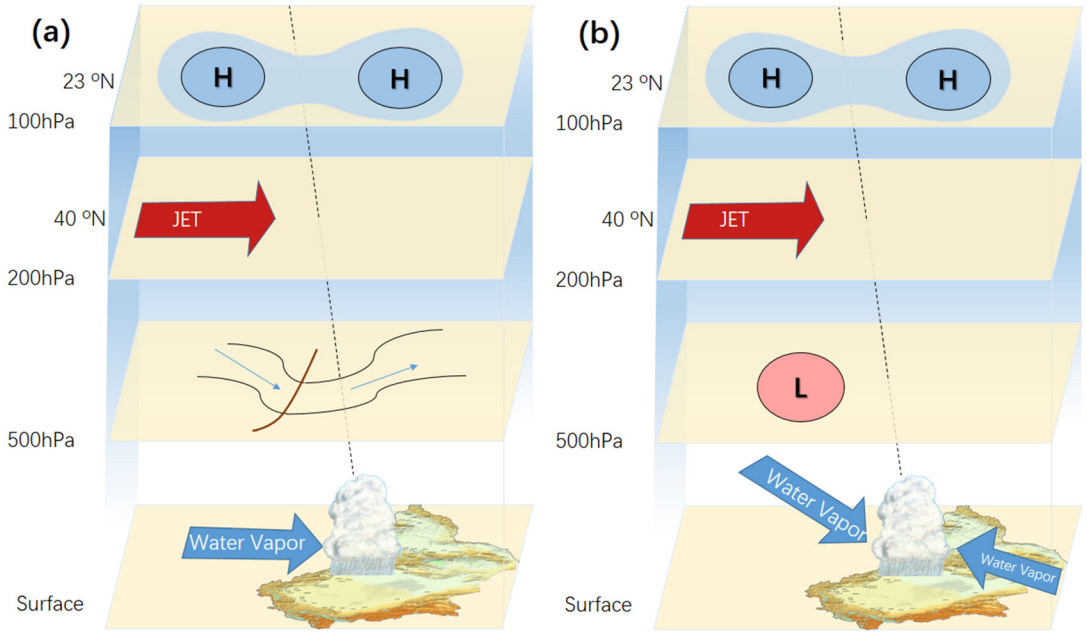

Figure 12. Conceptual model of (**a**) Type WT1 and (**b**) WT2. "H" represents the center of the high pressure. "L" represents the center of the low pressure. The black line represents the isobaric line. The brown line represents the trough line. The narrow blue arrow represents air flow. The latitudes on the left indicate the averaged location of the system on that level. The dotted black line represents the location of rainfall on the different levels.

On the other hand, three cases in Type WT are under the influence of vortexes at 500 hPa, and they all are similar to the typical case. The Central Asian vortex is one of the important influential systems causing heavy rain, short-term heavy precipitation, hail and sustained low temperature in Xinjiang [34–37]. Although these cases occur less frequently, they still should be discussed as configuration WT2 (Figure 12b). In configuration WT2, the vortex at 500 hPa on the west side of Lake Balkhash weakens and transforms into a trough during the eastward movement. The South Asia high still appears with two centers at 55° E and 95° E, respectively, while the westerly jet is located at 40° N. Water vapor enters Valley of Tianshan Mountains from the northwest and east sides of Xinjiang. Compared to configuration WT1, the influential system is a vortex in configuration WT2, and there is water vapor from the east.

In the three cases of Type NN, two were similar to the selected typical cases. In the typical configuration summarized (Figure 13a), the trough at 500 hPa was located in Siberia and moved eastward, while it appeared over the northern part of the Northern Xinjiang region on the extreme precipitation day. The South Asia High appeared with two centers at about 55° E and 85° E, respectively, while the westerly jet was located at 42° N. At the same time, there was a northwest jet over Xinjiang. Water vapor entered the northern part of the Northern Xinjiang region from the west and northwest of Xinjiang.

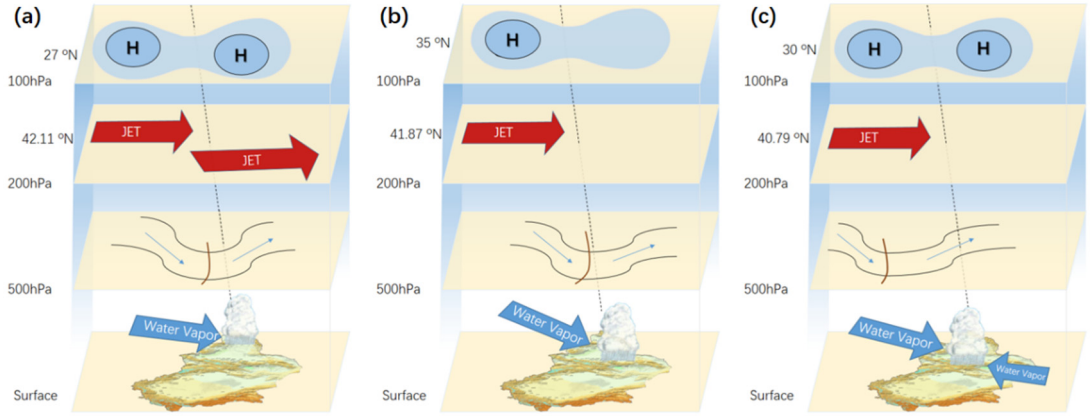

Figure 13. Conceptual model of (**a**) Type NN, (**b**) Type EN and (**c**) Type CT. "H" represents the center of the high pressure. The black line represents the isobaric line. The brown line represents the trough line. The narrow blue arrow represents air flow. The latitudes on the left indicate the averaged location of the system on that level. The dotted black line represents the location of rainfall on the different levels.

In the sixteen cases chosen as Type EN, nine cases were similar to the typical configuration (Figure 13b). The trough at 500 hPa was located in Siberia and moved eastward. On the extreme precipitation day, it appeared between Siberia and northeast Xinjiang. The South Asia High appeared as the Iran high pattern, with its center at about 60° E. The westerly jet was close to the Northern Xinjiang region. Water vapor came from the west and northwest of Xinjiang. Compared with Type NN, the influential system was located more eastward, and the South Asia High was located more northward and appeared as the Iran high pattern. The jet was located slightly southward, and the water vapor source was located more northward.

Finally, eight cases of Type CT were selected. Six of them were similar to the typical case (Figure 13c). In the typical configuration, the trough at 500 hPa at the south side of the vortex near 65° E in Siberia moved eastward, and it appeared between Lake Balkhash and the Aral Sea on the precipitation day. The South Asia High appeared with two centers, and its centers were located at about 60° E and 95° E. Compared with Type WT, the westerly jet was located more northward, and the water vapor entered the southern part of the Northern Xinjiang region from the east and northwest of Xinjiang. The influential system was positioned more westward in Type CT than in Type WT. The South Asia High was located more northward, while the jet was located slightly northward.

4. Summary and Discussion

Based on the daily precipitation in the Northern Xinjiang region in the summers of 1979–2018, 272 extreme precipitation days were defined. Using data on these days, the characteristics of extreme precipitation were investigated:

(1) Through principal component analysis on the precipitation data in the selected 272 days, 4 types of precipitation pattern were identified as the Western Tianshan Type (Type WT), north of Northern Xinjiang Type (Type NN), east of Northern Xinjiang Type (Type EN) and Eastern Tianshan Type (Type ET).

(2) Daily-averaged reanalysis data were used to compose and analyze the characteristics of related systems on the extreme precipitation day as well as the two days before and after. Geopotential data at 500 hPa were analyzed to determine that rainfall centers shifted with the troughs or vortexes at 500 hPa. Previous studies have already found similar results [12,38]. Then, the water vapor flux between the surface and 500 hPa was studied. In Type WT and Type NN, water vapor came from the west, but it mainly came from the east side in Type CT. In Type EN, water vapor converges from both sides. The different sources and trails of water vapor in the various types were consistent with previous studies [14–24,38]. Finally, the analysis of zonal wind speed data at 200 hPa indicates

that the upper-level jets in Type WT and Type CT are located west of 80° E. By contrast, in Type EN and Type NN, they were located east of 80° E. These jet stream characteristics are similar to previous findings [10–12,38].

(3) Based on the selected 40 cases, conceptual models of the four types of precipitation patterns are built. The South Asia High in Type EN exhibited the Iran high pattern, while in other types it exhibited a two-centers pattern. The upper-level jets in Types NN and Type EN were located more northward than in the case of the other two types. Low-pressure troughs appeared at 500 hPa near the Northern Xinjiang region in most models. The vortex acted as the influential system only in Type WT. In most cases, water vapor entered the Northern Xinjiang region from the west and northwest. However, the water vapor in type WT2 and CT came from the east. The positions of related systems in these models shared a resemblance with that of typical cases determined in previous forecast manuals [5,12].

Due to the significant differences in the climatic background between Southern and Northern Xinjiang, precipitation in these two areas needs to be analyzed separately. In the following research, we will use a similar method to analyze and determine the characteristics of extreme rainfall in southern Xinjiang.

Author Contributions: Data curation, R.X.; formal analysis, R.X., J.M.; investigation, R.X., J.M.; methodology, J.M.; project administration, J.M.; resources, R.X., J.M.; software, R.X.; supervision, J.M.; validation, R.X., J.M.; writing—original draft, R.X., J.M.; writing—review and editing, R.X., J.M. All authors have read and agreed to the published version of the manuscript.

Funding: This work was supported by the National Key R&D Program of China (2018YFC1507103), the National Natural Science Fund of China (41705032), the Doctoral Research Startup Foundation of Xinjiang University (50500/62031224618), and the 100 Young Doctors Introduction Program of Xinjiang (Tianchi Doctor Program) Foundation (50500/04231200737).

Data Availability Statement: Publicly available datasets were analyzed in this study. This data can be found here: https://www.ecmwf.int/en/forecasts/datasets/browse-reanalysis-datasets (accessed on 8 March 2021).

Acknowledgments: We thank Chenli Wang and Kun Zhao of Nanjing University for providing the assisting software for classification.

Conflicts of Interest: The authors declare no conflict of interest.

References

1. Huang, J.P.; Ran, J.J.; Ji, M.X. Preliminary analysis of the flood disaster over the arid and semi-arid regions in China. *Acta Meteorol. Sin.* **2014**, *72*, 1096–1107. (In Chinese)
2. Yang, L.M.; Li, X.; Zhang, G.X. Some Advances and Problems in the Study of Heavy Rain in Xinjiang. *Clim. Environ. Res.* **2011**, *16*, 188–198. (In Chinese)
3. Wang, N.; Cui, C.X.; Liu, Y. Temporal-spatial characteristics and the influencing factors of rainstorm-flood disasters in Xinjiang. *Arid Zone Res.* **2020**, *37*, 325–330. (In Chinese)
4. Geng, J.L.; Gao, L.; Chen, J.J. Analysis on the Hydrological in the Hutubi River Basin, Xinjiang. *Arid Zone Res.* **2005**, *22*, 371–376. (In Chinese)
5. Zhang, J.B.; Deng, Z.F. *Introduction to Precipitation in Xinjiang*, 1st ed.; China Meteorological Press: Beijing, China, 1987; pp. 315–322. (In Chinese)
6. Shi, Y.F.; Shen, Y.P.; Hu, R.J. Preliminary Study on Signal, Impact and Foreground of Climatic Shift from Warm-Dry to Warm-Humid in Northwest China. *J. Glaciol. Geocryol.* **2002**, *24*, 219–226.
7. Zhao, Y.; Wang, Q.; Huang, A. Relationship between Iran High Pattern of South Asia High and Summer Precipitation in Xinjiang. *Plateau Meteorol.* **2018**, *37*, 651–661.
8. Yang, L.M.; Zhang, Q.Y. Circulation characteristics of interannual and interdecadal anomalies of summer rainfall in north Xinjiang. *Chin. J. Geophys.* **2007**, *50*, 412–419. (In Chinese)
9. Zhang, Q.; Qian, Z.G.; Chen, M.H. The Further Study about South Asia High in Summer I. Statistic Analyses of Relationship between It and Precipitation Distribution Over Northwest China. *Plateau Meteorol.* **1997**, *16*, 52–62. (In Chinese)
10. Zhang, Y.C.; Kuang, X.Y.; Guo, W.D.; Zhou, T.J. Seasonal evolution of the upper-tropospheric westerly jet core over East Asia. *Geophys. Res. Lett.* **2006**, *33*, 317–324. [CrossRef]
11. Zhao, Y.; Wang, M.Z.; Huang, A.N.; Li, H.; Huo, W.; Yang, Q. Relationships between the West Asian subtropical westerly jet and summer precipitation in northern Xinjiang. *Theor. Appl. Climatol.* **2014**, *116*, 403–411. [CrossRef]

12. Zhang, J.B.; Su, Q.Y.; Sun, S.Q. *Guide Manual of Short Term Weather Forecast in Xinjiang*, 1st ed.; Xinjiang People's Publishing House: Xinjiang, China, 1986; p. 456. (In Chinese)
13. Wang, J.; Ren, Y.Y. Study on the Change of Precipitation and General Circulation in Xinjiang. *Arid Zone Res.* **2005**, *22*, 326–331. (In Chinese)
14. Wang, K.L.; Jiang, H.; Zhao, H.Y. Atmospheric water vapor transport from westerly and monsoon over the Northwest China. *Adv. Water Sci.* **2005**, *16*, 432–438. (In Chinese)
15. Liu, J.R.; Song, X.F.; Yuan, G.F.; Sun, X.M.; Liu, X.; Chen, F.; Wang, Z.M.; Wang, S.Q. Characteristics of $\delta^{18}O$ in precipitation over Northwest China and its water vapor sources. *Acta Geogr. Sin.* **2008**, *63*, 12–22. (In Chinese)
16. Huang, W.; Chang, S.Q.; Xie, C.L.; Zhang, Z.P. Moisture sources of extreme summer precipitation events in North Xinjiang and their relationship with atmospheric circulation. *Adv. Clim. Chang. Res.* **2017**, *8*, 12–17. [CrossRef]
17. Wang, X.R.; Xu, X.D.; Wang, W.G. Characteristic of spatial transportation of water vapor for Northwest China's rainfall in spring and summer. *Plateau Meteor.* **2007**, *26*, 749–758. (In Chinese)
18. Dai, X.G.; Li, W.J.; Ma, Z.G.; Wang, P. Water-vapor source shift of Xinjiang region during the recent twenty years. *Prog. Nat. Sci.* **2007**, *17*, 569–575.
19. Mason, S.J.; Goddard, L. Probabilistic precipitation anomalies associated with ENSO. *Bull. Am. Meteorol. Soc.* **2001**, *82*, 619–638. [CrossRef]
20. Mariotti, A.; Ballabrera-Poy, J.; Zeng, N. Tropical influence on Euro-Asian autumn rainfall variability. *Clim. Dyn.* **2005**, *24*, 511–521. [CrossRef]
21. Shi, Y.G.; Sun, Z.B.; Yang, Q. Characteristics of Area Precipitation in Xinjiang Region with Its Variations. *J. Appl. Meteorol. Sci.* **2008**, *19*, 326–332. (In Chinese)
22. Ao, J.; Sun, J.Q. Difference of water vapour transportation in the interannual and decadal variations of winter precipitation over western China. *Clim. Environ. Res.* **2014**, *19*, 497–506. (In Chinese)
23. Yang, L.M.; Zhang, Y.H.; Tang, H. Analyses on water vapor characteristic in three heavy rainstorm processes of Xinjiang in July 2007. *Plateau Meteor.* **2012**, *31*, 963–973. (In Chinese)
24. Zhang, Y.H.; Yu, B.X.; Wang, Z.K.; Jia, L.H. Dynamic mechanism and water vapor transportation characteristics of two extreme rainstorm events in Ili River valley in summer of 2016. *Torrential Rain Disasters* **2018**, *37*, 435–444. (In Chinese)
25. Dee, D.P.; Uppala, S.M.; Simmons, A.J.; Berrisford, P.; Poli, P.; Kobayashi, S.; Andrae, U.; Balmaseda, M.A.; Balsamo, G.; Bauer, P.; et al. The ERA-Interim reanalysis: Configuration and performance of the dataassimilation system. *Q. J. R. Meteorol. Soc.* **2011**, *137*, 553–597. [CrossRef]
26. Hersbach, H.; Bell, B.; Berrisford, P.; Hirahara, S.; Horányi, A.; Muñoz-Sabater, J.; Nicolas, J.; Peubey, C.; Radu, R.; Schepers, D.; et al. The ERA5 global reanalysis. *Q. J. R. Meteorol. Soc.* **2020**, *146*, 1999–2049. [CrossRef]
27. Zhao, Y.; Huang, A.; Zhou, Y.; Huang, D.; Yang, Q.; Ma, Y.; Li, M.; Wei, G. Impact of the Middle and Upper Tropospheric Cooling over Central Asia on the Summer Rainfall in the Tarim Basin, China. *J. Clim.* **2014**, *27*, 4721–4732. [CrossRef]
28. Richman, M.B. Rotation of principal components. *J. Climatol.* **1986**, *6*, 293–335. [CrossRef]
29. Huth, R. An intercomparison of computer-assisted circulation classification methods. *Int. J. Climatol. J. R. Meteorol. Soc.* **1996**, *16*, 893–922. [CrossRef]
30. Huth, R. Properties of the circulation classification scheme based on the rotated principal component analysis. *Meteorol. Atmos. Phys.* **1996**, *59*, 217–233. [CrossRef]
31. Li, M.; Zhang, Q.; Zhang, F. Hail day frequency trends and associated atmospheric circulation patterns over China during 1960–2012. *J. Clim.* **2016**, *29*, 7027–7044. [CrossRef]
32. Rao, X.; Zhao, K.; Chen, X.; Huang, A.; Xue, M.; Zhang, Q.; Wang, M. Influence of synoptic pattern and low-level wind speed on intensity and diurnal variations of orographic convection in summer over Pearl River Delta, South China. *J. Geophys. Res. Atmos.* **2019**, *124*, 6157–6179. [CrossRef]
33. Sun, J.H.; Zhao, S.X. The Impacts of Multiscale Weather Systems on Freezing Rain and Snowstorms over Southern China. *Weather Forecast.* **2010**, *25*, 388–407. [CrossRef]
34. Liu, Z.X.; Tian, H.P.; Zhao, J.R.; Wang, X.M. Analysis of the Cause for A Heavy Rain Happened Middle Tianshan Mountain in Xinjiang. *Desert Oasis Meteorol.* **2007**, *1*, 22–26. (In Chinese)
35. Zhang, J.W.; Liu, H.H.; Asima. Analysis of the Process for a Heavy Rain in Middle Tianshan Mountain on July 17th 2007. *Desert Oasis Meteorol.* **2008**, *2*, 18–21. (In Chinese)
36. Kong, Q.; Zheng, Y.G.; Chen, C.Y. Synoptic Scale and Mesoscale Characteristics of 7.17 Urumqi Heavy Rainfall in 2007. *J. Appl. Meteorol. Sci.* **2011**, *22*, 12–22. (In Chinese)
37. Zhuang, X.C.; Li, R.Q.; Li, B.Y.; Li, J.; Sun, Z.J. Analysis on Rainstorm Caused by Central Asian Vortex in Northern Xinjiang. *Meteorol. Mon.* **2017**, *43*, 924–935. (In Chinese)
38. Xie, Z.M.; Zhou, Y.S.; Yang, L.M. Review of study on precipitation in Xinjiang. *Torrential Rain Disasters* **2018**, *37*, 204–212. (In Chinese)